1 **Evaluation of cation exchange membrane performance under exposure to high Hg^0 and**
2 **HgBr$_2$ concentrations**

3 Matthieu B. Miller[1], Mae S. Gustin[2], Sarrah M. Dunham-Cheatham[2], Grant C. Edwards[1]

4 [1]Faculty of Science and Engineering, Department of Environmental Science, Macquarie University, Sydney, NSW,
5 2113, Australia
6
7 [2]Department of Natural Resources and Environmental Science, University of Nevada, Reno NV, 89557, United
8 States

10 *Correspondence to*: Matthieu B. Miller (matthieu.b.miller@gmail.com)

11 **Abstract**

12 Reactive mercury (RM) is an important component of the global atmospheric mercury cycle, but

13 measurement currently depends on un-calibrated, operationally defined methods with large

14 uncertainty and demonstrated interferences and artifacts. Cation exchange membranes (CEM)

15 provide a promising alternative methodology for quantification of RM, but method validation

16 and improvement are ongoing. For the CEM material to be reliable, uptake of gaseous elemental

17 mercury (GEM) must be negligible for all conditions, and RM compounds must be captured and

18 retained with high efficiency. In this study the performance of CEM material under exposure to

19 high concentrations of GEM ($1.43 \times 10^6 - 1.85 \times 10^6$ pg m^{-3}) and reactive gaseous mercury

20 bromide (HgBr$_2 \sim 5000$ pg m^{-3}) was explored, using a custom-built mercury vapor permeation

21 system, with quantification of total permeated Hg accomplished via pyrolysis at 600 °C and

22 detection using a Tekran® 2537A. Permeation tests were conducted for 24 to 72 hours in clean

23 laboratory air, with absolute humidity levels ranging from $0.1 - 10$ g m^{-3} water vapor. Gaseous

24 elemental mercury uptake by the CEM material averaged no more than 0.004% of total exposure

25 for all test conditions, which equates to a non-detectable GEM artifact for typical ambient air

26 sample concentrations. Recovery of HgBr$_2$ on CEM filters was >100 % compared to calculated

27 total permeated HgBr$_2$, suggesting incomplete thermal decomposition at the pyrolyzer, as the

28   CEM material collected $HgBr_2$ with less than 1% downstream breakthrough on average,

29   implying a high collection efficiency.

30

31   **1   Introduction**

32   Mercury (Hg) is a persistent environmental contaminant with a significant atmospheric life time,

33   and the form and chemistry of Hg is an important determinant of its biogeochemical cycling.

34   Mercury in the atmosphere is found in three forms: gaseous elemental mercury (GEM), gaseous

35   oxidized mercury (GOM), and particulate bound mercury (PBM). PBM and GOM are often

36   quantified together as reactive mercury (RM = GOM + PBM). Atmospheric GEM, at an average

37   global background concentration of $1 - 2$ ng m^{-3}, can be reliably measured with calibrated

38   analytical instruments (Gustin et al., 2015;Slemr et al., 2015). The measurement of GOM and

39   PBM requires detection at the part per trillion (pg m^{-3}) level and depends on un-calibrated

40   operationally defined methods with demonstrated interferences and artifacts, and concomitant

41   large uncertainty. Recent reviews (Gustin et al., 2015;Zhang et al., 2017) detail the

42   shortcomings, difficulties, and needed developments for atmospheric RM measurements.

43   As an alternative methodology, cation exchange membranes (CEM) have been used to

44   selectively measure GOM concentrations in ambient air (Huang et al., 2013;Huang and Gustin,

45   2015b;Huang et al., 2017;Sheu and Mason, 2001;Pierce and Gustin, 2017;Maruszak et al.,

46   2017;Ebinghaus et al., 1999;Mason et al., 1997;Bloom et al., 1996). The use of CEM type filters

47   for this purpose was first documented in the literature in a conference presentation (Bloom et al.,

48   1996), although such membranes (then referred to as 'ion exchange membranes') were deployed

49   earlier in a field-based international comparative study of RM measurement techniques in

50   September, 1995 (Ebinghaus et al., 1999). In the comparative study, one participating lab

51 deployed a series of ion exchange membranes (for GOM) behind a quartz fiber filter (for PBM)

52 at a sample flow rate of 9-10 Lpm, for 24 h measurements (filter pore sizes were not reported).

53 Results for PBM and GOM were in similar ranges of 4.5 – 26 pg m^{-3} and 13-23 pg m^{-3} ,

54 respectively (Ebinghaus et al., 1999).

55 The ion exchange membrane method was also applied in a 1995-96 field campaign for

56 determining the speciation of atmospheric Hg in the Chesapeake Bay area (Mason et al., 1997).

57 This study used a 5-stage Teflon filter pack system that included one up front quartz fiber filter

58 (0.8 μm pore size) to remove particulate, and four downstream Gelman ion exchange membranes

59 (pore size not reported) to 1) capture GOM, 2) capture GOM breakthrough, 3) serve as

60 deployment blanks, and 4) isolate the filter train on the downstream side (Mason et al., 1997).

61 Concentrations of GOM were reported to be 5 – 10 pg m^{-3}, essentially at or below the method

62 detection limit and it was speculated that even this small amount may have been an artifact from

63 fine particulate Hg passing through the 0.8 μm quartz fiber filter (Mason et al., 1997). The 3rd-in-

64 series ion exchange membrane blanks were reported to be not significantly different in Hg

65 concentration from unused membrane material, indicating that breakthrough was not a

66 phenomenon that extended past the second ion exchange filter position.

67 The particulate Hg artifact problem was subsequently elaborated on in a further comparative

68 study focusing exclusively on RM measurement techniques. Specific concerns included physical

69 particle breakthrough, re-evolution of gas-phase Hg^{2+} from PBM captured on the upstream

70 particulate filters passing downstream to the ion exchange membranes, possible adsorption of

71 GOM compounds to the particulate filters, or a GEM collection artifact on the ion exchange

72 membranes (Sheu and Mason, 2001). None of these concerns were proven or disproven

73 conclusively.

74 Recent CEM based sampling systems typically deploy a pair of CEM disc filters without a pre-

75 particulate filter, in replicates of 2 to 3 at a flow rate of 1.0 Lpm (Gustin et al., 2016). Each pair

76 of filters constitutes one sample, the first filter serving as the primary RM collection surface, and

77 the second filter capturing breakthrough. Filters are deployed for 1-to-2 weeks and then collected

78 for analysis (CVAFS, EPA Method 1631, modified) (Huang et al., 2017). The CEM material

79 consists of a positively charged polyethersulfone coated matrix (Pall Corporation), and at least

80 one manufacturing evolution has occurred (Huang and Gustin, 2015a). Prior CEM material

81 versions (I.C.E. 450) had a pore size of 0.45 μm, while the current CEM material (Mustang® S)

82 has a manufacturer reported pore size of 0.8 μm.

83 Previous work with the I.C.E 450 material indicated it does not adsorb significant quantities of

84 GEM in passive exposures, but can selectively uptake gas-phase Hg^{2+} species (Lyman et al.,

85 2007). The CEM material was subsequently adapted for use in active sample flow systems, with

86 the presumption of continued inertness to GEM and selectivity for GOM (Huang et al.,

87 2013;Huang and Gustin, 2015b). These studies and others (Lyman et al., 2016) have shown

88 better GOM recovery on CEM material compared to potassium chloride (KCl) coated denuder

89 methods.

90 Despite these tests, the transparency of the CEM material to GEM uptake has not been

91 conclusively demonstrated for active sampling flow rates, nor for high GEM concentrations,

92 though limited data using low concentration manual Hg^0 injections through CEM filters suggests

93 little or no GEM uptake (Lyman et al., 2016). However, even small rates of GEM uptake by the

94 CEM material could result in a significant measurement artifact (e.g. a modest $1 - 2\%$ GEM

95 uptake could easily overwhelm detection of typical ambient GOM concentrations). It is therefore

96 of critical importance that such a GEM artifact be ruled out if the CEM material is to be

97   successfully deployed for ambient RM measurements, first and foremost under controlled

98   laboratory conditions in the absence of confounding variables.

99   Additionally, previous studies have observed significant amounts of "breakthrough" GOM on the

100   secondary filter. The amount of breakthrough is not consistent, neither as a constant mass, with

101   total Hg ranging from zero to as high as 400 pg (Huang et al., 2017), nor as a percentage of Hg

102   collected on the primary filter, ranging from 0 – 40% (Pierce and Gustin, 2017). Similar variable

103   breakthrough issues were observed in the earliest field-based CEM measurements as well

104   (Mason et al., 1997). In contrast to ambient measurements, previous laboratory experiments have

105   reported only minor (0 – 16%) or no breakthrough (Huang et al., 2013;Huang and Gustin,

106   2015b). Limited experimental work with flow rates of 1.0 and 16.7 Lpm in ambient air could not

107   provide an explanation for differing breakthrough rates (Pierce and Gustin, 2017).

108   In this paper we investigate the potential for GEM uptake on CEM material using a custom-built

109   permeation system. In addition, the ability of the CEM material to capture and retain a

110   representative GOM compound (mercury bromide, $HgBr_2$) is discussed with a view to estimate

111   collection efficiency and explain or rule out possible mechanisms of breakthrough for both dry

112   and humid conditions.

113   **2   Methods**

114   A Tekran® 2537A ambient mercury analyzer was integrated with a custom-built permeation

115   system designed to enable controlled exposures of GEM and GOM to CEM filters (Fig. 1). The

116   2537A analyzer was calibrated at the beginning and periodically throughout the study and

117   checked for accuracy by manual Hg^0 injections (mean recovery 101.1% ± 4.3, n = 10, SI Fig. 1).

118   The entire system was checked for Hg contamination in clean air prior to permeation tests, and

119   periodically during sampling (SI Fig. 2). All tubing and connections used in the permeation

120   system were polytetrafluoroethylene (PTFE), except for the quartz glass pyrolyzer tube and

121   perfluoroalkoxy (PFA) filter holders. Each of these materials is known to be chemically inert,

122   virtually nonporous, and to have a low coefficient of friction. For these reasons, PTFE/PFA

123   plastic and quartz glass are the standard materials employed in almost all Hg sampling systems,

124   as GEM passes over or through these surfaces without loss (Gustin et al., 2015). Given its

125   reactive nature, some GOM inevitably adsorbs to internal line surfaces, but the capacity of these

126   materials to sorb and retain GOM is not infinite and a steady state of adsorption/desorption is

127   expected after 5-6 hours of exposure to a stable concentration (Xiao et al., 1997;Gustin et al.,

128   2013).

129   Sample flow through the system was alternated between two PTFE sample lines (designated

130   Line 0 and Line 1) using a Tekran® Automated Dual Switching (TADS) unit. Sample air was

131   constantly pulled through each line at 1.0 Lpm by the internal pump and mass flow controller in

132   the 2537A, or by an external flush pump (KNF Laboport® N86 KNP) and mass flow controller

133   (Sierra Smart-Trak® 2). Laboratory air was pulled through a single inlet at the combined rate of

134   2.0 Lpm, passing through a 0.2 µm PTFE particulate filter and an activated charcoal scrubber to

135   produce clean sample air. Additionally, for dry air permeations sample air was pulled through a

136   Tekran® 1102 Air Dryer installed upstream of the particulate filter, and for elevated humidity

137   permeations sample air was pulled through the headspace of a distilled water bath (DIW, < 0.2

138   ng L^{-1} total Hg) that was located upstream from the charcoal scrubber to eliminate the DIW being

139   a potential Hg source to the system. Temperature and relative humidity (RH) were measured in-

140   line (Campbell Scientific CS215) and used for calculation of absolute humidity.

141   Pure liquid Hg^0 and crystalline $HgBr_2$ (purity > 99.998% Sigma-Aldrich®) were used as Hg

142   vapor sources. The elemental Hg^0 bead was contained in a PTFE vial. Solid $HgBr_2$ crystals were

143   packed in thin-walled PTFE heat-shrink tubing (O.D. 0.635 cm) with solid Teflon plugs in both

144   ends to create a perm tube with an active permeation length of 2 mm (Huang et al., 2013). The

145    $HgBr_2$ permeation tube was also placed in the bottom of a PTFE vial, and the permeation vials

146   were submerged in a temperature-controlled laboratory chiller (0.06 ± 0.13 °C, Cole Parmer

147   Polystat®). A low source temperature was favored both because higher temperatures would have

148   produced unacceptably high concentrations, and because there is evidence that at higher

149   temperatures a small amount of Hg^0 can be evolved from Hg^{2+} compounds (Xiao et al., 1997).

150   An ultra-high purity nitrogen (N_2) carrier gas was passed through the permeation vials at 0.2

151   Lpm to carry the target Hg vapor into the main sample line through a PTFE T-junction. The main

152   sample line was split into Line 0 and Line 1 immediately downstream from the permeation flow

153   junction. Line 0 proceeded directly to the 2537A without modification during GEM permeations

154   (Fig. 1A), but housed CEM filters during the $HgBr_2$ permeations (Fig. 1B, 1C). Line 1 held a

155   pyrolyzer unit composed of a quartz glass tube (O.D. 0.625 cm) packed with a 3 cm section of

156   quartz wool heated to 600 °C using a nichrome wire coil (SI Fig. 3 and discussion). The goal of

157   the pyrolyzer was to convert all Hg to GEM for detection on the Tekran® 2537A.

158   CEM filters were deployed in 2-stage, 47 mm disc PFA filter holders (Savillex©). The primary

159   "A" filter in the 2-stage holder is the first to be exposed to the permeated Hg, with the secondary

160   "B" filter mounted immediately behind the A filter (A to B distance ~ 3mm) to measure potential

161   breakthrough. For GEM permeations, three 2-stage filter holders were placed in-series on Line 1

162   behind the pyrolyzer unit (Fig. 1A), while total Hg coming through the system was measured on

163   Line 0 with no filters in place. This allowed simultaneous exposure of 6 CEM filters in one GEM

164   sample exposure. The first CEM filter in-line served to scrub any small residual RM passing

165   through the system and pyrolyzer, and these first in-line filters were removed for the calculations

166   of GEM uptake (SI Fig. 4 and discussion).

167   For determining the potential for GOM breakthrough, two system configurations were used. In

168   the first configuration (Fig. 1B), the total Hg concentration of air that passed through the

169   pyrolyzer on Line 1 was measured without any filters, while Line 0 held one 2-stage CEM filter

170   pair for $HgBr_2$ loading. This configuration allowed for real time (10 min interval) quantification

171   of the $HgBr_2$ permeation concentration through Line 1 using the 2537A, and comparison with

172   total Hg loading on the CEM filters on Line 0. In the second configuration, replicate filters were

173   concurrently loaded with $HgBr_2$ by placing 2-stage CEM filter holders on both Line 0 and Line 1

174   (upstream of the pyrolyzer, Fig. 1C). In all $HgBr_2$ exposures, the filter holders were placed as

175   close to the permeation vial as possible, with a total distance from vial to filter surface of

176   approximately 20 cm. Mercury bromide permeation was conducted in dry air and elevated

177   humidity air. The difference between one line being fully open to the $HgBr_2$ permeation flow

178   (configuration Fig. 1B) and then closed by deployment of the CEM filters (configuration Fig.

179   1C) enabled a rough determination of the amount of $HgBr_2$ line-loss within the system.

180   After permeation, CEM filters were collected into clean, sterile polypropylene vials and analyzed

181   for total Hg by digestion in an oxidizing acid solution, reduction to Hg^0, gold amalgamation, and

182   final quantification by cold vapor atomic fluorescence spectrometry (CVAFS, EPA Method

183   1631, Rev. E) using a Tekran® 2600 system. This analysis provided for comparison of total Hg

184   filter loading, and verification of in-line results. A to B filter breakthrough was calculated by

185   comparison of total Hg recoveries on the primary and secondary CEM filters, using Eq. (1):

186 $$\% \; Breakthrough = 100 * CEM_{2nd}/(CEM_{1st} + CEM_{2nd}) \; (1)$$

187 Blank CEM filters were collected and analyzed in the same manner with every set of sample

188 filters deployed on the permeation system, and the mean filter blank value was subtracted from

189 all total Hg values to calculate the final blank-corrected Hg values used for data analysis. All

190 data were analyzed in Microsoft® Excel (version 16.12) and RStudio® (version 3.2.2).

191 **3   Results**

192 **3.1 Elemental Mercury Uptake on CEM Filters**

193 Elemental Hg uptake on CEM material was negligible for permeated Hg^0 vapor concentrations

194 ranging from $1.43{\times}10^6 - 1.85{\times}10^6$ pg m^{-3} (Fig. 2). High GEM concentrations were employed in

195 this study under the logic that if no GEM uptake was observed at high concentrations, a similar

196 lack of GEM uptake can be expected for all lower concentrations.

197 The mean Hg mass on blank CEM filters was 50 ± 20 pg (n = 28). For permeations into dry

198 sample air of 0.5 ± 0.1 g m^{-3} water vapor (WV), total mean Hg^0 permeation exposures of $2.7{\times}10^6$

199 pg (24 h) and $7.3{\times}10^6$ pg (72 h) resulted in total (blank-corrected) Hg recoveries on the CEM

200 filters of 100 ± 40 pg (n = 10) and 280 ± 110 pg (n = 5), respectively. These quantities of total

201 recovered Hg equate to a mean GEM uptake rate on the CEM filters of $0.004 \pm 0.002\%$. For

202 GEM permeations into ambient humidity sample air ($2 - 4$ g m^{-3} WV), at a slightly lower total

203 mean permeated Hg^0 24 h exposure of $2.1{\times}10^6$ pg, total (blank-corrected) Hg recoveries on the

204 CEM filters were 55 ± 30 pg (n =10), equating to a GEM uptake rate of $0.003 \pm 0.001\%$. The

205 overall GEM uptake rate was linear ($r^2 = 0.97$) for the range of concentrations used in this study,

206 indicating a similar low uptake rate can be expected down to lower GEM concentrations.

3.2 Mercury Bromide Uptake on CEM Filters

Breakthrough of $HgBr_2$ vapor from the primary (A) to secondary (B) CEM filters was low for all

conditions tested in this study (Table 1). These conditions included $HgBr_2$ permeated into clean

dry laboratory air with < 0.5 g m^{-3} WV, clean air at ambient room humidity ($4 - 5$ g m^{-3} WV),

and clean air at elevated humidity ($10 - 11$ g m^{-3} WV), at line temperatures between 17 to 19 °C.

Overall, the mean A to B filter breakthrough ranged from 0 to 0.5% and averaged 0.2 ± 0.2 % (n

= 17), with no statistical difference observed in mean breakthrough rates for the three levels of

humidity (ANOVA, $p = 0.124$).

The first $HgBr_2$ permeation in clean dry (< 0.5 g m^{-3} WV) laboratory air was over a 96 h period,

using the system configuration in Figure 1B to establish an approximately permeation rate (Fig.

3). Total Hg reaching the 2537A through the pyrolyzer on Line 1 (red line, Fig. 3) indicates an

average $HgBr_2$ exposure concentration of 4540 pg m^{-3}, or about 4.5 pg min^{-1} from the permeation

tube. After this permeation, total blank-corrected $HgBr_2$ loading on the primary CEM filter on

Line 0 was 49400 pg, but only 50 pg on the secondary CEM filter, indicating a breakthrough rate

of approximately 0.1%. Total Hg reaching the 2537A through the CEM filters on Line 0 (black

line, Fig. 3) over this time period was 15 pg, mostly at the beginning of the deployment when

some ambient Hg entered the opened system. The low concentrations of Hg measured

downstream in Line 0 on the 2537A corroborates that breakthrough of $HgBr_2$ was low. These

data also demonstrate that the CEM material did not saturate with a $HgBr_2$ loading of ~ 50000

pg, a loading far higher than could be expected in ambient conditions.

Subsequent replicate 24 h $HgBr_2$ permeations in clean dry air resulted in consistent total Hg

loading on CEM filters placed on both lines concurrently (8560 ± 320 pg, n = 6, Samples 2-7

229 Table 1), and mean total Hg on the secondary CEM filters was 20 ± 10 pg (average

230 breakthrough of 0.3%). On Line 0 (black line, Fig.3), which was never open to $HgBr_2$ vapor

231 downstream from the CEM filters at any point in the study, Hg measured at the 2537A was zero

232 for all three 24 h permeations, indicating no breakthrough (Samples 2, 4, & 6, Table 1).

233 However, on Line 1, which had been exposed to the full $HgBr_2$ vapor concentration of 4540 pg

234 m^{-3} over the duration of the 96 h perm test, 1155 pg of Hg were measured downstream in the first

235 24 h sample (Sample 3, Table 1). The amount of downstream Hg dropped to 10 pg in the second

236 24 h, and 6 pg in the third 24 h (Samples 5 & 7, Table 1). This downstream Hg in Line 1

237 (compared to the zero Hg simultaneously observed on Line 0) is attributed to re-volatilization of

238 $HgBr_2$ that had stuck to the line material during the open permeation flow. At the moment CEM

239 filters were deployed on Line 1 (red-to-blue transition, Fig. 3), a rapid asymptotic decline in the

240 Hg signal began. This decay curve supports drawdown and depletion of a Hg reservoir on the

241 interior line surfaces behind the CEM filters, and not a continuous source such as breakthrough

242 from the permeation tube that was still supplying $HgBr_2$ to both sample lines. The total mass of

243 Hg re-volatized from the interior line surfaces (1155 pg) represents 4 − 5% of the total $HgBr_2$ that

244 had passed through Line 1 (~25000 pg based on 2537A measurement). Eventually, Hg reaching

245 the 2537A through Line 1 decreased to zero during the same 24 h filter deployment, indicating a

246 majority of $HgBr_2$ line contamination can be expected to flush out within ~12 h.

247 Additional $HgBr_2$ permeations were made at two levels of in-line humidity. At ambient room

248 humidity (4 − 5 g m^{-3} WV), mean total Hg measured on the CEM filters was 7910 ± 520 pg (n =

249 4; Samples H2-5, Table 1), with an average breakthrough to the secondary filters of 0.3%. When

250 normalized for sample volume, the mean $HgBr_2$ loading on CEM filters during ambient humidity

251 (5968 ± 125 pg) and dry air (5995 ± 188 pg) permeations was not statistically significantly

252   different (t-test $p = 0.790$). $HgBr_2$ breakthrough rates were also the same (0.3%) as during the

253   dry air permeations, indicating that the permeation system was operating similarly at the two

254   humidity levels, and suggesting that absolute humidity concentrations around $4 – 5$ g m^{-3} WV

255   have insignificant effects on collection of $HgBr_2$ in clean laboratory air by the CEM material.

256   We observed that an increase in humidity resulted in an initial large increase in Hg measured at

257   the 2537A downstream of the CEM filters on Line 0 (Sample H1, Table 1), concurrently with an

258   open $HgBr_2$ permeation flow through Line 1 while both lines were subjected to increased RH.

259   This downstream Hg on Line 0 dropped substantially to zero in ~10 h in the first 24 h

260   deployment (Sample H2, Table 1), and was zero for the duration of the second 24 h deployment

261   (Sample H4, Table 1). As this downstream Hg rapidly declined to zero, we believe this was also

262   an off-gassing effect, likely induced by the increased humidity, which perhaps facilitated a

263   heterogeneous surface reduction of $HgBr_2$ to GEM in the short section of line between the perm

264   source and CEM filters, with the GEM then passing through to the 2537A. As the breakthrough

265   rate and the mean $HgBr_2$ loading on the CEM filters did not change between the dry air and

266   ambient humidity permeations, the downstream Hg observed at the 2537A during the ambient

267   humidity permeations cannot be attributed to a loss of Hg from the CEM filters and is more

268   likely due to a process in the sample lines.

269   As a further test of possible humidity effects, two replicate 24 h CEM filter deployments were

270   conducted in elevated humidity conditions ($10 – 11$ g m^{-3} WV) created by an in-line water bath.

271   Mean total Hg loading on the primary CEM filters was higher compared to the previous

272   permeations (11700 ± 720 pg, $n = 4$, Samples H9-12, Table 1), indicating an increase in the

273   effective $HgBr_2$ permeation rate, possibly due to the perturbation caused by a poor filter seal and

274   small leak in the preceding deployment (Sample H7-8, Table 1). However, mean total Hg on the

275   secondary CEM filters was 20 ± 20 pg, indicating an average breakthrough of 0.1%, less than the

276   breakthrough observed for the lower humidity permeations.

277   **4   Conclusions**

278   GEM uptake on the CEM material was negligible under the laboratory conditions and high GEM

279   loading rates (2 orders of magnitude above ambient) tested in this study, with an overall linear

280   uptake rate of 0.004% for permeated GEM concentrations between $1.43 \times 10^6 - 1.85 \times 10^6$ pg m^{-3}.

281   This uptake rate would be insignificant at typical ambient atmospheric Hg concentrations (1 – 2

282   ng m^{-3}). As a hypothetical example, a CEM filter sampling ambient air at an average GEM

283   concentration of 2 ng m^{-3} for a typical 2-week sample period would have a total Hg^0 exposure of

284   ~40000 pg. At the calculated uptake rate of 0.004%, a maximum 1.6 pg of Hg observed on the

285   sample filter could be attributed to GEM artifact and given that blank filters have a mean total

286   Hg mass of 50 ± 20 pg, this amount would be below detection. This corroborates the lack of

287   GEM uptake seen by Lyman et al. (2016) for manual Hg^0 injections on CEM filters at lower total

288   mass loadings of 300 – 6000 pg.

289   Mean HgBr$_2$ breakthrough from primary to secondary CEM filters averaged 0.2 ± 0.2% over all

290   test conditions, using HgBr$_2$ as a test GOM compound. A to B filter breakthrough was derived

291   from a comparison between the large amount of HgBr$_2$ permeated onto the primary CEM filters,

292   to the small amount of HgBr$_2$ that collected on the secondary CEM filters, 3 mm immediately

293   downstream. The measurement of 1000s of pg of Hg on the primary filter, and only 10s of pg on

294   the secondary filter, leads to the conclusion that the primary filter removed the majority of HgBr$_2$

295   from the sample air stream. In addition, low breakthrough was corroborated by downstream

296   measurement of the air stream passing through the CEM filters, using the Tekran® 2537A. The

297 average breakthrough to the 2537A was 0 pg for 24 h permeations in dry air and 0 – 40 pg in

298 humid air, for those filter deployments than can be considered steady-state (> 24 h without large

299 perturbations).

300 While the permeation system was not specifically optimized for a quantitative mass balance

301 between permeated $HgBr_2$ and $HgBr_2$ recovered on the CEM filters, a rough estimation of the

302 CEM collection efficiency is possible. Using the $HgBr_2$ permeations conducted in clean dry air

303 (mean loading 8560 pg) and comparing this to the mean Hg concentration measured at the

304 2537A analyzer during the last 24 h of the 96 h permeation measurement (4680 pg m^{-3}, or 6739

305 pg per 24 h), the $HgBr_2$ recovery on the CEM filters averaged 127%. Adjusting the expected

306 permeated $HgBr_2$ mass for our estimated line-loss (~4-5%) improves the recoveries to ~123%.

307 Still, $HgBr_2$ loading on the CEM filters was therefore ~23% higher than expected based on the

308 pyrolized total measurement on the 2537A.

309 The technique of gold amalgamation in general, and specifically including the Tekran® 2537

310 analyzer, is widely considered to provide a quantitative *total gaseous Hg* measurement, at or

311 very near 100% collection efficiency for Hg^0 and Hg compounds (Dumarey et al.,

312 1985;Schroeder and Jackson, 1985;Landis et al., 2002;Temme et al., 2003;Schroeder et al.,

313 1995). However, to our knowledge collection and desorption efficiencies on gold traps have not

314 been demonstrated for $HgBr_2$. The stated desorption temperature of the Tekran® 2537A gold

315 traps is 500 °C, but temperatures as low as 375 °C have been reported (Gustin et al., 2013),

316 which would likely cause reduced thermal decomposition efficiency for all captured GOM

317 compounds, including $HgBr_2$. We speculate that a combination of incomplete thermal

318 decomposition to Hg^0, at both the 600 °C pyrolyzer and during the best-case 500 °C desorption

319   of the 2537 gold traps, resulted in ~20% non-detection of total permeated $HgBr_2$ as it passed

320   through the CVAFS optical path without generating the necessary fluorescence signal.

321   While our results validated some basic performance metrics for the CEM material, they did not

322   provide data that could fully explain the higher levels of breakthrough observed for CEM filters

323   deployed in ambient air over the 1 to 2 week sample periods in previous studies. Increasing

324   humidity by itself did not affect observed $HgBr_2$ breakthrough. A $HgBr_2$ loading of ~50000 pg

325   also did not lead to increased breakthrough, indicating there is no saturation effect on CEM filter

326   capacity at a GOM loading far greater than expected from ambient concentrations. It remains

327   unclear, though, whether breakthrough results from different collection efficiencies for GOM

328   compounds other than $HgBr_2$, or whether breakthrough results from a degradation of GOM

329   retention capacity in the CEM material when exposed to ambient air chemistries not simulated in

330   this study. Also, our experiments were conducted in particulate-free air, which leaves open the

331   possibility that breakthrough is related to capture (or lack thereof) of PBM by the CEM material.

332   **Acknowledgements**

333   The authors would like to acknowledge funding from Macquarie University iMQRES 2015148

334   and NSF Grant 629679, as well as valuable input and assistance from Dr. Ashley Pierce, Dr. Seth

335   Lyman, and the students of Dr. Gustin's laboratory.

336
337
338
339
340
341
342
343
344
345

References

Bloom, N., Prestbo, E., and VonderGeest, E.: Determination of atmospheric gaseous Hg(II) at the pg/m 3 level by collection onto cation exchange membranes, followed by dual amalgamation/cold vapor atomic fluorescence spectrometry, 4th International Conference on Mercury as a Global Pollutant, Hamburg, 1996.

Dumarey, R., Dams, R., and Hoste, J.: Comparison of the collection and desorption efficiency of activated charcoal, silver, and gold for the determination of vapor phase atmospheric mercury, Analytical Chemistry, 57, 2638-2643, 10.1021/ac00290a047, 1985.

Ebinghaus, R., Jennings, S. G., Schroeder, W. H., Berg, T., Donaghy, T., Guentzel, J., Kenny, C., Kock, H. H., Kvietkus, K., Landing, W., Muhleck, T., Munthe, J., Prestbo, E. M., Schneeberger, D., Slemr, F., Sommar, J., Urba, A., Wallschlager, D., and Xiao, Z.: International field intercomparison measurements of atmospheric mercury species at Mace Head, Ireland, Atmospheric Environment, 33, 3063-3073, 1999.

Gustin, M. S., Huang, J., Miller, M. B., Peterson, C., Jaffe, D. A., Ambrose, J., Finley, B. D., Lyman, S. N., Call, K., Talbot, R., Feddersen, D., Mao, H., and Lindberg, S. E.: Do We Understand What the Mercury Speciation Instruments Are Actually Measuring? Results of RAMIX, Environmental Science & Technology, 47, 7295-7306, 10.1021/es3039104, 2013.

Gustin, M. S., Amos, H. M., Huang, J., Miller, M. B., and Heidecorn, K.: Measuring and modeling mercury in the atmosphere: a critical review, Atmos. Chem. Phys., 15, 5697-5713, 10.5194/acp-15-5697-2015, 2015.

Gustin, M. S., Pierce, A. M., Huang, J., Miller, M. B., Holmes, H. A., and Loria-Salazar, S. M.: Evidence for Different Reactive Hg Sources and Chemical Compounds at Adjacent Valley and High Elevation Locations, Environmental Science & Technology, 50, 12225-12231, 10.1021/acs.est.6b03339, 2016.

Huang, J., Miller, M. B., Weiss-Penzias, P., and Gustin, M. S.: Comparison of Gaseous Oxidized Hg Measured by KCl-Coated Denuders, and Nylon and Cation Exchange Membranes, Environmental Science & Technology, 47, 7307-7316, 10.1021/es4012349, 2013.

Huang, J., and Gustin, M. S.: Use of Passive Sampling Methods and Models to Understand Sources of Mercury Deposition to High Elevation Sites in the Western United States, Environmental Science & Technology, 49, 432-441, 10.1021/es502836w, 2015a.

Huang, J., and Gustin, M. S.: Uncertainties of Gaseous Oxidized Mercury Measurements Using KCl-Coated Denuders, Cation-Exchange Membranes, and Nylon Membranes: Humidity Influences, Environmental Science & Technology, 49, 6102-6108, 10.1021/acs.est.5b00098, 2015b.

Huang, J., Miller, M. B., Edgerton, E., and Sexauer Gustin, M.: Deciphering potential chemical compounds of gaseous oxidized mercury in Florida, USA, Atmos. Chem. Phys., 17, 1689-1698, 10.5194/acp-17-1689-2017, 2017.

384 Landis, M. S., Stevens, R. K., Schaedlich, F., and Prestbo, E. M.: Development and
385 characterization of an annular denuder methodology for the measurement of divalent inorganic
386 reactive gaseous mercury in ambient air, Environmental Science & Technology, 36, 3000-3009,
387 10.1021/es015887t, 2002.

388 Lyman, S., Jones, C., O'Neil, T., Allen, T., Miller, M., Gustin, M. S., Pierce, A. M., Luke, W.,
389 Ren, X., and Kelley, P.: Automated Calibration of Atmospheric Oxidized Mercury
390 Measurements, Environmental Science & Technology, 50, 12921-12927,
391 10.1021/acs.est.6b04211, 2016.

392 Lyman, S. N., Gustin, M. S., Prestbo, E. M., and Marsik, F. J.: Estimation of Dry Deposition of
393 Atmospheric Mercury in Nevada by Direct and Indirect Methods, Environmental Science &
394 Technology, 41, 1970-1976, 10.1021/es062323m, 2007.

395 Marusczak, N., Sonke, J. E., Fu, X., and Jiskra, M.: Tropospheric GOM at the Pic du Midi
396 Observatory—Correcting Bias in Denuder Based Observations, Environmental Science &
397 Technology, 51, 863-869, 10.1021/acs.est.6b04999, 2017.

398 Mason, R., Lawson, N., and Sullivan, K.: The concentration, speciation and sources of mercury
399 in Chesapeake Bay precipitation, Atmospheric Environment, 31, 3541-3550, 10.1016/S1352-
400 2310(97)00206-9, 1997.

401 Pierce, A. M., and Gustin, M. S.: Development of a Particulate Mass Measurement System for
402 Quantification of Ambient Reactive Mercury, Environmental Science & Technology, 51, 436-
403 445, 10.1021/acs.est.6b04707, 2017.

404 Schroeder, W., and Jackson, R.: An instrumental analytical technique for speciation of
405 atmospheric mercury, International Journal of Environmental Analytical Chemistry, 22, 1-18,
406 10.1080/03067318508076405, 1985.

407 Schroeder, W., Keeler, G., Kock, H., Roussel, P., Schneeberger, D., and Schaedlich, F.:
408 International field intercomparison of atmospheric mercury measurement methods, Water Air
409 and Soil Pollution, 80, 611-620, 10.1007/BF01189713, 1995.

410 Sheu, G. R., and Mason, R. P.: An examination of methods for the measurements of reactive
411 gaseous mercury in the atmosphere, Environmental Science & Technology, 35, 1209-1216,
412 10.1021/es001183s, 2001.

413 Slemr, F., Angot, H., Dommergue, A., Magand, O., Barret, M., Weigelt, A., Ebinghaus, R.,
414 Brunke, E., A Pfaffhuber, K., Edwards, G., Howard, D., Powell, J., Keywood, M., and Wang, F.:
415 Comparison of mercury concentrations measured at several sites in the Southern Hemisphere,
416 3125-3133 pp., 2015.

417 Temme, C., Einax, J. W., Ebinghaus, R., and Schroeder, W. H.: Measurements of Atmospheric
418 Mercury Species at a Coastal Site in the Antarctic and over the South Atlantic Ocean during
419 Polar Summer, Environmental Science & Technology, 37, 22-31, 10.1021/es025884w, 2003.

420   Xiao, Z., Sommar, J., Wei, S., and Lindqvist, O.: Sampling and determination of gas phase
421   divalent mercury in the air using a KCl coated denuder, Fresenius Journal of Analytical
422   Chemistry, 358, 386-391, 1997.

423   Zhang, L., Lyman, S., Mao, H., Lin, C. J., Gay, D. A., Wang, S., Sexauer Gustin, M., Feng, X.,
424   and Wania, F.: A synthesis of research needs for improving the understanding of atmospheric
425   mercury cycling, Atmos. Chem. Phys., 17, 9133-9144, 10.5194/acp-17-9133-2017, 2017.

426

427
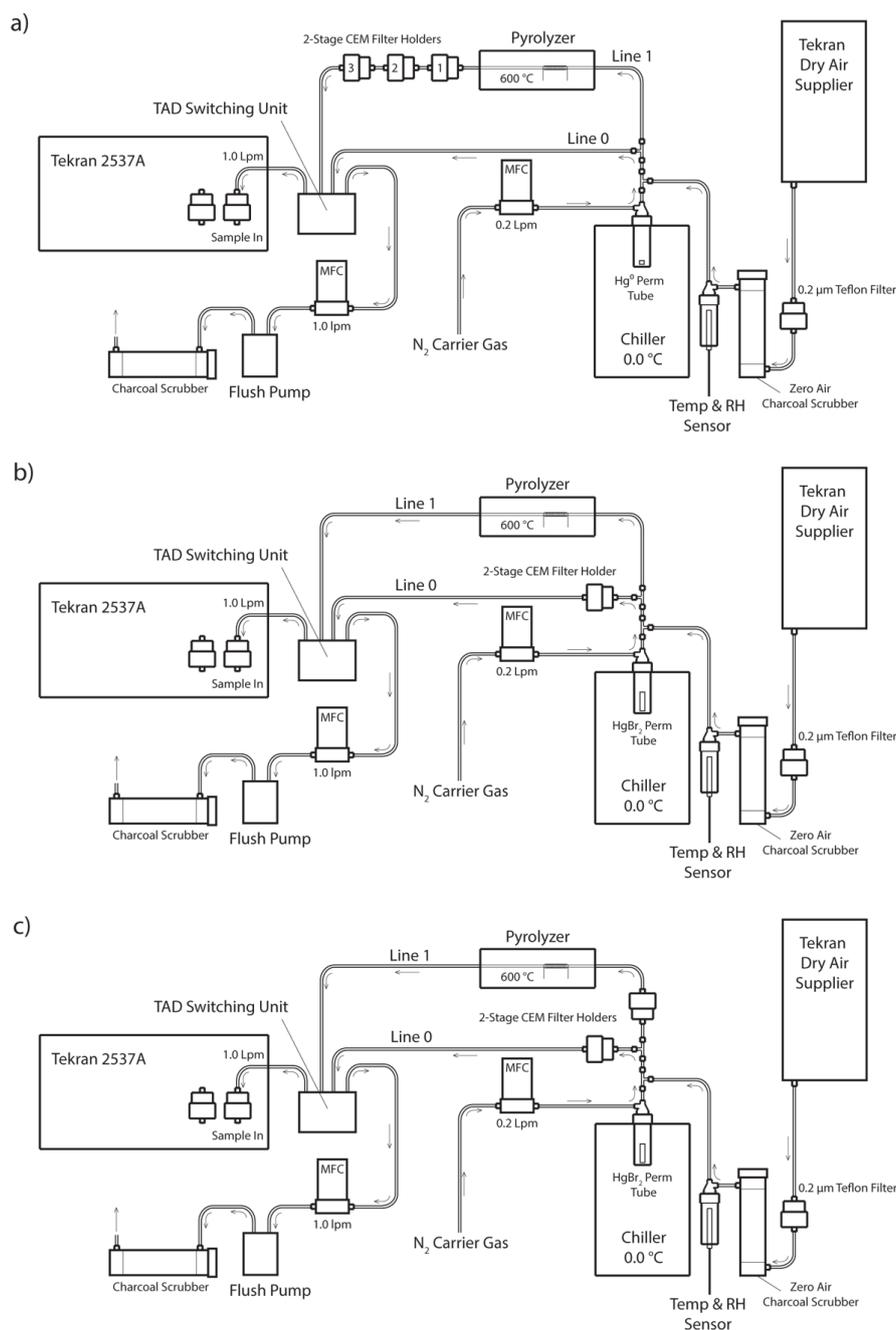
Figure 1. Schematic of the Hg vapor permeation system configurations for: a) GEM permeations b) HgBr$_2$
permeations c) Simultaneous HgBr$_2$ loading on two sample lines. Note dry air supplier disconnected for ambient and
elevated humidity HgBr$_2$ permeations, with sample path starting at 0.2 μm Teflon particulate filter and water bath
inserted immediately in front of the charcoal scrubber. All tubing is chemically inert PTFE, except for the quartz
glass pyrolyzer tube, and PFA filter holders.

433
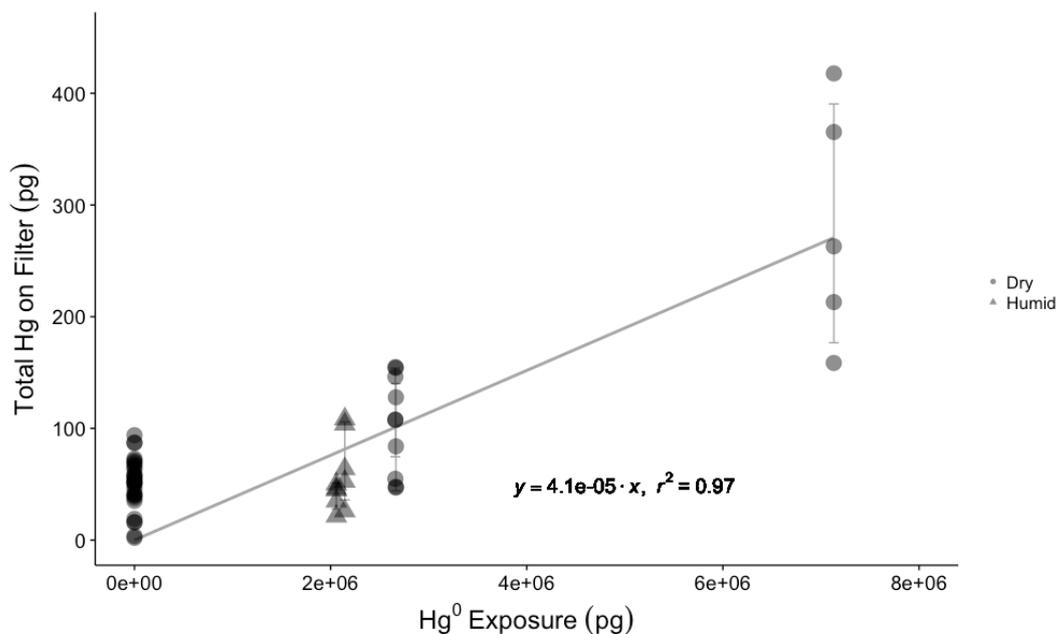
Figure 2. Total Hg recovered on CEM material for blank filters (Hg exposure = 0 pg) and different Hg^0 vapor
permeations in dry (0.5 ± 0.1 g m^{-3} WV) and humid air (2-4 g m^{-3} WV). Circles represent dry air permeations,
triangles represent humid air exposures, and all permeation exposures were blank-corrected. The regression line
shows the relationship between total Hg^0 exposure and blank-correct mean total Hg recovered on CEM filters (error
bars ± one standard deviation), with a slope of 4.1×10^{-5} indicating a linear uptake rate of 0.004%.

439

440

441

442
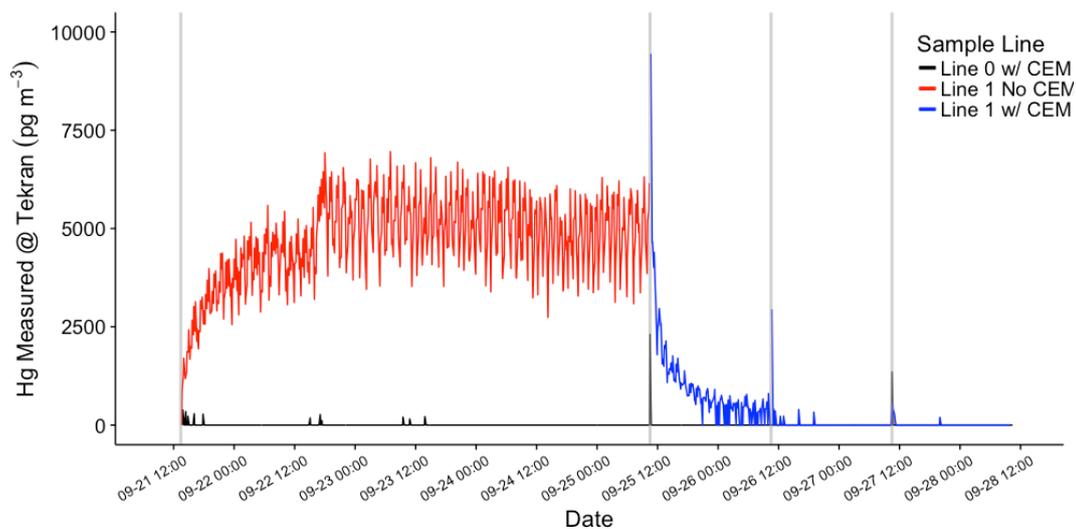
443
444   **Figure 3**. HgBr₂ permeations in clean dry lab air using the configuration in Figure 1B (red line) and Figure 1C (blue
445   line). The red line indicates total Hg released from permeation tube and passing through pyrolyzer on Line 1 before
446   being measured by Tekran 2537A, black line indicates Hg reaching 2537A through CEM filters on Line 0. Vertical
447   grey lines indicate open system during filter deployments.

448

449

450

451

452

453

454

455

456

457

458

459

460

461

Table 1.

Sample	Start	End	Sample Time (min)	Sample Flow (lpm)	Sample Volume (m³)	Total Hg on CEM (pg)	Blank Correct (pg)	Total Hg @ Tekran (pg)	A to B Filter Brkthru (%)
Mean CEM Filter Blank							54		
Clean Dry Air (0.3 ± 0.05 g m⁻³ wv)									
HgBr 1P	*9/21/17 13:25*	*9/25/17 10:25*	*5580*	*1.00*	*5.580*	*na*	*na*	*25181*	*na*
HgBr 1A	9/21/17 13:25	9/25/17 10:25	5580	1.00	5.580	49478	49424	15	0.10
HgBr 1B						101	47		
HgBr 2A	9/25/17 10:30	9/26/17 10:30	1440	1.00	1.440	8901	8847	0	0.20
HgBr 2B						71	17		
HgBr 3A	*9/25/17 10:30*	*9/26/17 10:30*	*1440*	*1.00*	*1.440*	*9125*	*9072*	*1155*	*0.36*
HgBr 3B						*86*	*33*		
HgBr 4A	9/26/17 10:40	9/27/17 10:25	1425	1.00	1.425	8494	8440	0	0.28
HgBr 4B						77	24		
HgBr 5A	*9/26/17 10:40*	*9/27/17 10:25*	*1425*	*1.00*	*1.425*	*8306*	*8253*	*10*	*0.36*
HgBr 5B						*83*	*29*		
HgBr 6A	9/27/17 10:35	9/28/17 10:25	1430	1.00	1.430	8496	8442	0	0.22
HgBr 6B						72	19		
HgBr 7A	*9/27/17 10:35*	*9/28/17 10:05*	*1410*	*1.00*	*1.410*	*8386*	*8333*	*6*	*0.15*
HgBr 7B						*66*	*13*		
Clean Humid Air (4.4 ± .2 g m⁻³ wv)									
HgBr H1P	*10/2/17 16:10*	*10/3/17 15:20*	*1390*	*1.00*	*1.390*	*na*	*na*	*5888*	*na*
HgBr H1A	10/2/17 16:10	10/3/17 15:20	1390	1.00	1.390	10498	10444	1700	0.25
HgBr H1B						80	27		
HgBr H2A	10/3/17 15:30	10/4/17 14:40	1390	1.00	1.390	8589	8535	164	0.13
HgBr H2B						65	11		
HgBr H3A	*10/3/17 15:30*	*10/4/17 14:40*	*1390*	*1.00*	*1.390*	*8182*	*8129*	*420*	*0.54*
HgBr H3B						*98*	*44*		
HgBr H4A	10/4/17 14:50	10/5/17 11:50	1260	1.00	1.260	7504	7451	0	0.31
HgBr H4B						76	23		
HgBr H5A	*10/4/17 14:50*	*10/5/17 11:50*	*1260*	*1.00*	*1.260*	*7576*	*7522*	*25*	*0.25*
HgBr H5B						*73*	*19*		
HgBr H6P	*10/5/17 12:05*	*10/9/17 10:25*	*5660*	*1.00*	*5.660*	*na*	*na*	*11889*	*na*
HgBr H7A	10/9/17 10:40	10/10/17 10:45	1445	1.00	1.445	9024	8970	105	na
HgBr H7B						2672*	2618*		
HgBr H8A	*10/9/17 10:40*	*10/10/17 10:45*	*1445*	*1.00*	*1.445*	*12359*	*12305*	*397*	*na*
HgBr H8B						*75*	*21*		
Clean High Humidity Air (10.9 ± 1.7 g m⁻³ wv)									
HgBr H9A	10/10/17 10:50	10/11/17 9:30	1360	1.00	1.360	10920	10866	181	0.22
HgBr H9B						78	24		
HgBr H10A	*10/10/17 10:50*	*10/11/17 9:30*	*1360*	*1.00*	*1.360*	*11413*	*11359*	*308*	*0.00*
HgBr H10B						*53*	*0*		
HgBr H11A	10/11/17 9:35	10/12/17 9:35	1440	1.00	1.440	12001	11947	5	0.00
HgBr H11B						52	0		
HgBr H12A	*10/11/17 9:35*	*10/12/17 9:35*	*1440*	*1.00*	*1.440*	*12579*	*12525*	*40*	*0.29*
HgBr H12B						*90*	*36*		
HgBr H13P	*10/12/17 9:40*	*10/13/17 9:40*	*1440*	*1.00*	*1.440*	*na*	*na*	*1430*	*na*
HgBr H13A	10/12/17 9:40	10/13/17 9:40	1440	1.00	1.440	13152	13099	4	0.12
HgBr H13B						69	16		

462

463 **Table 1.** Summary of CEM filter loading and breakthrough during HgBr₂ permeations. Samples denoted P indicate
464 approximate permeation rate check through Line 1 via pyrolyzer and Tekran 2537A, italics indicate filter
465 deployments on Line 1, and * indicates high values due to leak around first filter seal.